

Carbohydrate microarrays for the recognition of cross-reactive molecular markers of microbes and host cells

Denong Wang*, Shaoyi Liu, Brian J. Trummer, Chao Deng, and Aili Wang

We describe here the development of a carbohydrate-based microarray to extend the scope of biomedical research on carbohydrate-mediated molecular recognition and anti-infection responses. We have demonstrated that microbial polysaccharides can be immobilized on a surface-modified glass slide without chemical conjugation. With this procedure, a large repertoire of microbial antigens (~20,000 spots) can be patterned on a single micro-glass slide, reaching the capacity to include most common pathogens. Glycoconjugates of different structural characteristics are shown here to be applicable for microarray fabrication, extending the repertoires of diversity and complexity of carbohydrate microarrays. The printed microarrays can be air-dried and stably stored at room temperature for long periods of time. In addition, the system is highly sensitive, allowing simultaneous detection of a broad spectrum of antibody specificities with as little as a few microliters of serum specimen. Finally, the potential of carbohydrate microarrays is demonstrated by the discovery of previously undescribed cellular markers, Dex-Ids.

The surface of a mammalian cell is decorated with complex carbohydrates, existing as glycoconjugates of different molecular configurations, such as glycoproteins, glycolipids, glycosaminoglycans, and proteoglycans. Expression of these molecules, especially their carbohydrate structures, is frequently specific to cell or tissue type, and in many cases, restricted to specific stages of cellular differentiation and development^{1,2}. Cellular glycoconjugates play important roles in many biological processes, including events of molecular recognition at fertilization^{3,4} and processes of cell–cell recognition, adhesion, and cell activation throughout the development and maturation of a living organism^{1,2,5,6}. Abnormalities in the expression of complex carbohydrates are found in cancer^{7,8}, retrovirus infection^{9,10}, and other diseases¹¹. Deciphering the information content of cellular glycomers is a current focus in the developing field of glycomics⁵.

Carbohydrate structures also play critical roles in host–microorganism interactions. Many host receptors or co-receptors for microbes are glycoconjugates¹²; their structural diversity and selectivity of host tissue expression contribute significantly to the tropism of microbial infections^{12,13}. On the other hand, polysaccharides and other microbe-derived molecules serve as the main antigenic structures which host cells recognize and mount a response to¹⁴. A number of cases have been documented in which microbial antigens mimic the structures of host components, assisting a microbe to escape from a host's immune defense^{15,16}. Such mimicking microbial antigens may also induce autoimmune disorders, contributing to the pathogenesis of an infectious disease^{13,15}. Identification and characterization of such antigenic structures may lead to a better understanding of the biological relationship between host and microorganism as well as the molecular mechanisms of infectious diseases.

We aimed to develop a carbohydrate-based microarray system to extend the scope of biomedical research on carbohydrate-mediated molecular recognition. This could also allow simultaneous detection of a wide range of microbial infections using limited quantities of clinical specimen. In this report, we investigate several critical technical questions that determine the feasibility of establishing a carbohydrate-based microarray. These include (1) whether carbohydrate macromolecules of hydrophilic character can be immobilized on a glass surface by methods that are suitable for high-throughput production of microarrays; (2) whether immobilized carbohydrate-containing macromolecules preserve their immunological properties, such as expression of carbohydrate epitopes or antigenic determinants and their solvent accessibility; (3) whether the carbohydrate microarray system reaches the sensitivity and capacity to detect a broad range of antibody specificities in clinical specimens; and (4) whether this technology can be applied to investigate the carbohydrate-mediated molecular recognition on a scale that was previously impossible.

Results and discussion

A model system for establishing carbohydrate microarray technology. The dextrans and anti-dextran antibodies^{14,17} were applied to establish methods for immobilizing carbohydrate polymers on glass slides. Dextrans are polymers composed entirely of glucose, produced mainly by bacteria of the family Lactobacillaceae and of the genera *Leuconostoc* and *Streptococcus*. Dextran molecules derived from different strains may, however, differ significantly in their glycosidic linkage compositions. Unlike proteins that are linked solely by a peptide bond, carbohydrates utilize many possible glycosidic linkages so as to diversify their structures extensively. Some dextran

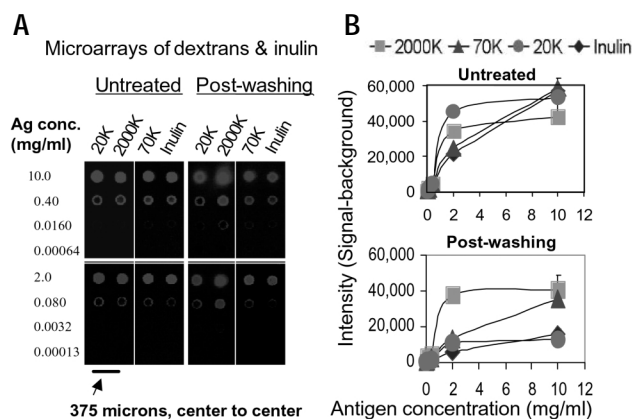


Figure 1. Immobilization of polysaccharides on a nitrocellulose-coated glass slide. (A) Image of the carbohydrate microarray spots before and after washing. (B) Quantitative illustration of the relation of fluorescence intensity and the concentration of printed carbohydrate microarrays before and after washing. Fluorescent conjugates of dextrans or inulin were dissolved in saline (0.9% NaCl) and spotted at an initial concentration of 10 mg/ml and then diluted in serial dilutions of 1:5. The microarray slides were scanned before and after washing. Data of six repeats of the same experiment were statistically analyzed and presented in (B).

preparations are predominantly or solely $\alpha(1,6)$ -linked, forming molecules with dominantly linear chain structures; others are composed of multiple glycosidic linkages, including $\alpha(1,6)$ -, $\alpha(1,3)$ -, $\alpha(1,2)$ -, and others, generating heavily branched molecules¹⁸ (Table 1). Previous immunological studies^{17,19} have demonstrated that such structural characteristics are detectable by antibodies specific for different antigenic determinants or epitopes of dextran molecules. This system is, therefore, suitable for developing methods for immobilization of carbohydrate antigens and for investigating their immunological properties in a surface-immobilized configuration.

We applied the fluorescein isothiocyanate (FITC)-conjugated polysaccharides as probes to investigate whether nitrocellulose-coated glass slides can be used to immobilize microspots of carbohydrate polymers without covalent conjugation. FITC- $\alpha(1,6)$ dextran preparations of different molecular weights and a structurally distinct polysaccharide, inulin, were printed on the glass slides using a microprinting device to produce a carbohydrate microarray (Fig. 1A). Their fluorescent signals were then captured and quanti-

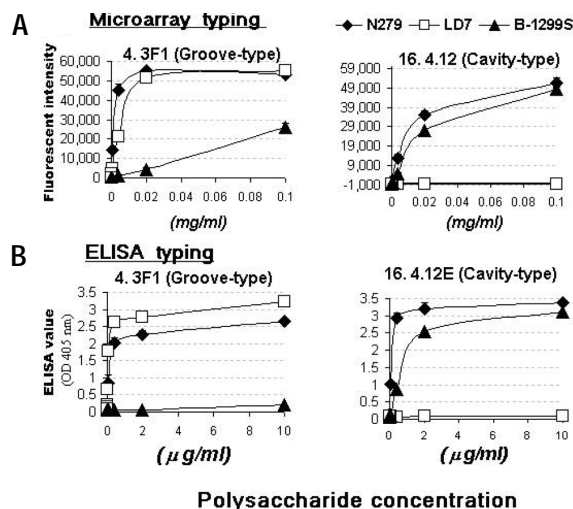


Figure 2. Immunological characterization of surface-immobilized dextran molecules. (A) Microarray binding curves of a groove-type anti-Dex 4.3F1 (IgG3/Kappa) and a cavity-type anti-dextran 16.4.12E (IgA/Kappa) to dextran molecules of distinct structure. Dextran molecules were printed with an initial concentration of 0.1 mg/ml and diluted by a 1:5 series titration. The printed arrays were washed to remove unbound antigens and then stained with biotinylated anti-dextran, either 4.3F1 or 16.4.12E, at a concentration of 1 μ g/ml, and then stained with Cy3-streptavidin at 1:500 dilutions. The readout of the experiment (i.e., fluorescent intensity of the microspot) reflects the amounts of antigen immobilized and epitopes displayed for antibody recognition. The cavity-type mAb 16.4.12E bound to N279 and B1299S, but not LD7. By contrast, the groove-type mAb 4.3F1 bound to the dextran preparations N279 and LD7, but bound poorly to B1299S. (B) ELISA binding curve of anti-Dex 4.3F1 and 16.4.12E. Dextran preparations were coated on an ELISA plate at an initial concentration of 10 μ g/ml and then diluted by a 1:5 series titration in 0.02 M borate-buffered saline, pH 8.0. The antigen-coated plates were incubated with biotinylated anti-dextrans at a concentration of 1 μ g/ml. The bound antibodies were revealed with an alkaline phosphatase (AP)-streptavidin conjugate and AP substrate.

fied by a microscanning system that was developed for scanning complementary DNA (cDNA) microarrays. By analyzing the fluorescent intensities retained on the slides after extensive washing, we demonstrated that dextran preparations ranging from 20 kDa to 2,000 kDa and inulin of 3.3 kDa were all stably immobilized on the nitrocellulose-coated slide without chemical conjugation. The effi-

Table 1. Structural properties of dextrans and inulin preparations

	Plain dextrans			FITC conjugates			
	N279	LD7	B1299S	Dex-20K	Dex-70K	Dex-2000K	Inulin
Structural characteristics							
Molecular weight (kDa)	~10,000	42	~20,000	19.6	71.2	2,000	3.2
Sugar residue	Glucose	Glucose	Glucose	Glucose	Glucose	Glucose	Fructose
Conformational characteristics	Linear chain	Linear chain	Heavily branched	Linear chain	Linear chain	Linear chain	Linear chain
Molar ratio (FITC:sugar)	0	0	0	0.01	0.005	0.008	0.007
Proportions of linkages (%)^a							
$\alpha(1,6)$ Terminal nonreducing end group	5	0	31	5	5	5	0
$\alpha(1,6)$ Backbone	90	100	32	90	90	90	0
$\alpha(1,3)\alpha(1,6)$ Backbone	0	0	1	0	0	0	0
$\alpha(1,2)\alpha(1,6)$ Backbone	0	0	5	0	0	0	0
$\alpha(1,3)$ Branches	5	0	1	5	5	5	0
$\alpha(1,2)$ Branches	0	0	30	0	0	0	0
$\beta(2,1)$ Linkage	0	0	0	0	0	0	100 (?)

^aValues are estimated from methylation and periodate-oxidation analysis (see ref. 18 for a summary).

Table 2. Microarray detection and characterization of human and murine anti-carbohydrate antibodies^a

Antigen microspots				I. Human IgM			II. Human IgG			III. Anti-Dex 4.3F1			IV. Anti-Dex 16.4.12E		
Antigen name	Class ^b	ID	Location	Mean	s.d.	Int./Bk. ^c	Mean	s.d.	Int./Bk.	Mean	s.d.	Int./Bk.	Mean	s.d.	Int./Bk.
<i>Klebsiella</i> type 7	1	1	A1	19,293	1,786	1.12	32,140	3,367	3.86	9,074	215	1.01	11,432	324	1.02
<i>Klebsiella</i> type K11	1	2	A2	19,560	3,349	1.13	15,262	7,630	1.52	9,584	837	1.06	11,432	262	1.03
<i>Klebsiella</i> type K13	1	3	A3	39,103	4,354	2.17	25,997	719	3.20	23,003	3,573	2.56	12,256	648	1.10
<i>Klebsiella</i> type K21	1	4	A4	22,847	2,131	1.27	29,255	890	3.63	8,817	203	0.98	12,487	367	1.12
Dudmans <i>Rhizobium</i> TA1	1	5	A5	31,625	2,768	1.77	16,198	693	2.06	8,438	448	0.93	10,901	226	0.98
Chondroitin sulfate "B"	2	6	A6	17,009	633	0.96	10,830	411	1.40	59,264	822	6.38	18,063	935	1.62
<i>Pneumococcus</i> type C	1	7	C1	17,014	1,661	0.98	25,187	3,499	3.02	8,813	373	0.98	11,256	271	1.00
<i>Pneumococcus</i> type VIII	1	8	C2	17,194	1,407	0.98	12,075	3,754	1.47	8,862	362	0.99	11,450	512	1.02
<i>Pneumococcus</i> type XIV	1	9	C3	17,012	1,262	0.96	12,292	4,286	1.52	8,879	330	0.99	11,359	375	1.02
Cow 21 (blood group B)	3	10	C4	19,336	2,180	1.08	9,280	839	1.15	9,020	325	1.00	11,309	450	1.02
Bacto-agar 20°C Ext	1	11	C5	19,792	2,512	1.09	9,682	1,276	1.20	9,106	251	1.02	11,269	527	1.02
Arabino galactan (Larch)	1	12	C6	16,216	453	0.90	8,599	474	1.08	8,564	433	0.97	10,909	357	0.99
IM3-BSA ^d	4	13	E1	19,743	1,898	1.11	14,322	1,750	1.70	10,490	258	1.17	65,535	0	5.34
IM3-KLH ^d	4	14	E2	18,077	1,185	1.01	10,641	930	1.27	8,629	390	0.98	62,128	5069	5.42
Le ^a (N-110% 2x)	3	15	E3	17,046	728	0.95	8,960	605	1.08	8,742	287	1.00	11,026	501	0.98
Beach P1 (blood group B)	3	16	E4	17,419	525	0.97	10,022	423	1.21	8,638	307	0.96	10,928	561	0.97
Tij II (blood group B and Le ^a)	3	17	E5	17,946	464	0.99	9,400	503	1.14	8,556	202	0.95	11,006	457	0.98
OG ^d	3	18	E6	20,682	2,620	1.13	8,819	459	1.08	8,912	427	1.00	11,148	705	0.99
ASOR ^d	3	19	G1	16,555	449	0.93	8,933	320	1.06	8,627	547	0.96	10,923	566	1.00
LNT-BSA ^d	4	20	G2	19,053	1,266	1.05	9,010	287	1.08	8,509	497	0.96	11,000	316	0.99
Phosphomannan	1	21	G3	17,571	785	0.97	16,124	923	1.93	8,585	483	0.96	11,224	394	1.01
<i>Meningococcus</i> group B	1	22	G4	16,747	620	0.93	8,839	403	1.06	8,633	285	0.96	11,115	623	0.99
<i>Haemophilus influenzae</i> type A	1	23	G5	17,804	656	0.98	11,007	208	1.33	8,637	378	0.95	11,205	499	1.01
<i>Escherichia coli</i> K92	1	24	G6	17,353	770	0.95	8,785	328	1.07	8,714	396	0.97	11,248	190	1.01
<i>Klebsiella</i> type A3	1	25	I1	27,018	9910	1.40	13,001	6,947	1.94	10,278	1,120	1.12	11,496	136	1.01
<i>Klebsiella</i> type K12	1	26	I2	32,322	16,450	1.69	11,539	5,029	1.72	9,303	293	1.01	11,504	226	1.01
<i>Klebsiella</i> type K14	1	27	I3	23,360	1283	1.22	54,557	2,045	7.80	9,687	343	1.04	11,752	405	1.03
<i>Klebsiella</i> type K33	1	28	I4	54,607	2574	2.60	22,890	1,259	3.37	16,135	3,620	1.70	11,286	424	1.00
Chondroitin sulfate "A"	2	29	I5	18,093	1252	0.99	7,646	730	1.16	9,443	451	1.01	11,322	215	1.00
Chondroitin sulfate "C"	2	30	I6	17,699	983	0.97	7,547	607	1.14	11,936	3,057	1.35	11,810	396	1.05
<i>Pneumococcus</i> type SIV	1	31	K1	19,002	662	1.00	11,485	819	1.68	9,305	351	1.03	11,388	94	1.00
<i>Pneumococcus</i> type IX	1	32	K2	18,932	1303	1.00	10,600	3,827	1.56	9,345	697	1.02	11,407	227	1.01
<i>Pneumococcus</i> type 27	1	33	K3	23,308	6222	1.24	13,455	7,158	1.97	9,104	914	1.00	11,394	252	1.00
Cow26 (blood group B)	3	34	K4	19,184	1743	1.03	8,020	885	1.19	9,296	916	1.01	11,309	205	1.00
<i>Helix pomatia</i> galactan	1	35	K5	17,885	722	0.97	7,298	550	1.11	9,186	917	0.99	11,369	268	1.01
<i>Helix nemoralis</i> galactan	1	36	K6	18,135	715	0.98	7,412	416	1.10	9,179	773	0.98	11,234	185	1.00
IM6-BSA ^d	4	37	M1	18,897	184	1.01	9,991	784	1.41	10,610	423	1.13	62,509	2,863	5.43
IM6-KLH ^d	4	38	M2	17,761	289	0.96	7,857	544	1.13	9,303	250	1.00	13,534	460	1.19
Le ^a (N-1 IO ₄ NaOH)	3	39	M3	18,430	926	1.00	7,857	626	1.11	9,223	216	0.98	11,293	240	1.00
Cyst 9 (blood group A)	3	40	M4	18,182	552	0.99	9,081	733	1.30	9,129	333	0.98	11,571	689	1.04
Dextran N-150-N (60K)	1	41	M5	17,527	717	0.96	7,908	671	1.17	57,385	1,630	6.02	12,653	197	1.13
Hog (blood group H)	3	42	M6	17,791	1,015	0.98	7,706	506	1.13	9,604	288	1.01	11,526	145	1.04
AGOR ^d	3	43	O1	18,218	305	0.98	7,698	485	1.09	9,228	384	0.99	11,327	360	1.00
Inulin	1	44	O2	17,655	361	0.95	7,636	326	1.08	9,274	391	0.99	11,264	511	1.00
Levan (B-512E)	1	45	O3	18,003	318	0.97	11,807	2,116	1.68	9,493	190	1.00	11,423	521	1.01
<i>Meningococcus</i> group Y	1	46	O4	17,278	841	0.95	7,749	433	1.09	9,158	80	0.97	11,454	687	1.01
<i>E. coli</i> K1	1	47	O5	17,518	1,219	0.97	7,442	508	1.11	9,193	222	0.97	11,236	364	1.00
<i>E. coli</i> K100	1	48	O6	17,852	807	0.99	15,823	2,152	2.33	9,157	163	0.96	11,178	270	1.00
Background (n = 200)				18,267	844		7,522	727		9,161	356		11,252	365	
Total number of positives:						12			35			4			4

^aData of four microarrays were statistically analyzed and the positive results are emphasized with **bold italics**. For human serum antibody staining, a positive score is given if the mean fluorescent intensity value of a microspot is significantly higher than the mean background of the identically stained microarray with the same fluorescent color. For the staining using mAbs, a positive score is given if the mean fluorescent intensity value of a microspot is at least 1.5-fold higher than the mean background.

^bCarbohydrate antigens were classified and indicated in the table as follows: 1, polysaccharide; 2, glycosaminoglycan; 3, glycoprotein; 4, semisynthetic glycoconjugate.

^cInt./Bk., Ratio of mean fluorescence intensity to mean background.

^dAGOR, agalacto-orosomucoid; ASOR, Asialo-orosomucoid; IM, isomaltose oligosaccharide; KLH, keyhole limpet hemocyanin; LNT, lacto-N-tetraose; OG, Ogunshye 10% 2X (blood group I activity).

bodies in human serum when the amount of specimen is limited. The system therefore allows probing repertoires of human antibodies with anti-carbohydrate activities and characterizing a wide range of microbial infections. In addition, identification of a broad spectrum of human anti-carbohydrate antibodies of IgG isotype (Fig. 3) indicates that the isotype profile of anti-carbohydrate antibodies in normal individuals may differ from those in the repertoires of human

myeloma and lymphoma proteins. In our previous long-term effort, led by the late Professor Elvin A. Kabat (Columbia University), more than 2,000 cases of human myeloma, lymphoma, or benign human monoclonal gammopathy were screened by gel diffusion assay, resulting in the identification of a panel of 46 anti-carbohydrate monoclonals^{14,23-26}. The samples were randomly collected from clinics based solely on the detection of a monoclonal spike on electrophoresis,



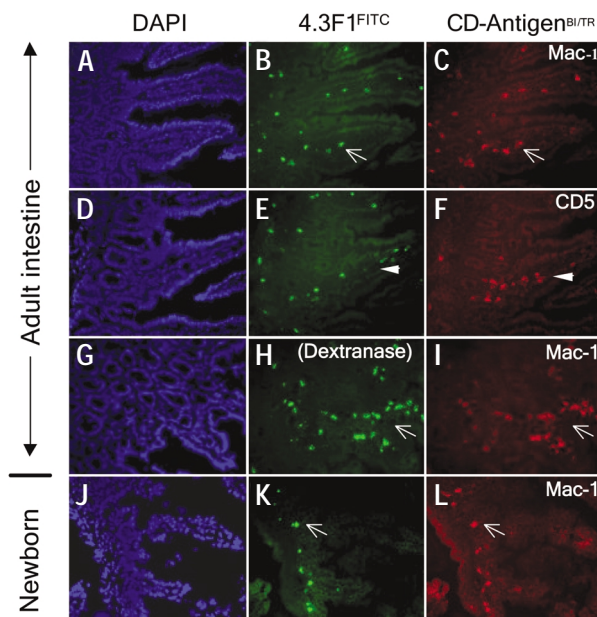


Figure 4. An anti- $\alpha(1,6)$ dextran antibody cross-reacts with intestinal MAC1⁺ cells. The cryostat sections of small intestine were co-stained with mAb 4.3.F1^{FITC} (IgG3) and a biotinylated antibody recognizing a known cellular marker. DAPI staining was applied to visualize the overall tissue structure. The three-color fluorescence staining was visualized by using corresponding filters. In the adult mouse, the 4.3.F1⁺ cells are co-stained by an anti-MAC1 and are widely distributed in the lamina propria of small intestine. The 4.3.F1 staining is resistant to the pretreatment of tissue by dextranase. In the newborn mouse, the double-positive cells were, however, detected in a restricted area: the base region but not the long-tip region of villi. A mouse IgG3 isotype standard mAb with anti-KLH specificity, A12-3^{FITC} (BD-PharMingen), showed no staining of the MAC1⁺ cell population as expected (data not shown). (A–C, adult) Co-staining of (A) DAPI (B) 4.3.F1^{FITC}, and (C) MAC1^{BI/avidin}Tex Red. (D–F, adult) Co-staining of (D) DAPI (E) 4.3.F1^{FITC}, and (F) CD5^{BI/avidin}Tex Red. (G–I, adult) Tissue was pretreated with dextranase and then stained with (G) DAPI (H) 4.3.F1^{FITC}, and (I) MAC1^{BI/avidin}Tex Red. (J–L, newborn) Co-staining of (J) DAPI (K) 4.3.F1^{FITC}, and (L) MAC1^{BI/avidin}Tex Red.

including different antibody isotypes. These human anti-carbohydrate antibodies were, however, exclusively of the IgM isotype. Apparently, our microarray data challenges a current belief that naturally occurring anti-polysaccharide antibodies are mainly of IgM “natural antibody” type²⁷, which were thought to be produced by a specific B-lymphocyte subset (B-1 cells)²⁸.

Characterizing specificity and cross-reactivity of carbohydrate/anti-carbohydrate interaction. Given the large potential of carbohydrate microarrays, we propose that this system can extend the scope of our investigation on the specificity and cross-reactivity of carbohydrate–receptor interactions. Examples of carbohydrate-mediated antibody cross-reactivities were previously reported; some were proven to be of biological and medical significance^{13,15,16,29,30}. To test this possibility, two anti-dextran mAbs of well-characterized combining sites, 4.3.F1 and 16.4.12E, were applied to interact with a large panel of carbohydrate antigens on the microarray (Fig. 3). The binding of 16.4.12E (cavity-type) but not 4.3.F1 (groove-type) to isomaltotriose-coupled BSA (IM3-BSA) and IM3-keyhole limpet hemocyanin (IM3-KLH) (Fig. 3A, III and IV, E1 and E2) reflects epitope-specific binding activities of the two mAbs. The groove-type anti- $\alpha(1,6)$ dextran 4.3F1, however, showed significant cross-reactivity to chondroitin sulfate B polysaccharide (CS-B) (Fig. 3A, III, A6), which was unexpected. The CS-B preparation is derived from porcine intestinal mucosa. Its predominant structure, the repeating disaccharide sequence of 4-sulfated N-

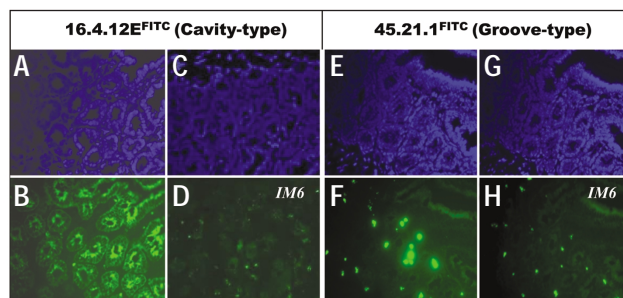


Figure 5. Groove-type and cavity-type anti- $\alpha(1,6)$ dextran antibodies recognize distinct cellular markers. The cryostat sections of small intestine were stained with either the cavity-type anti- $\alpha(1,6)$ dextran mAb 16.4.12E^{FITC} (IgA) (A–D) or the groove-type mAb 45.21.1^{FITC} (IgA) (E–H), in the presence (C, D, G, and H) or absence (A, B, E, and F) of specific competitor, oligosaccharide IM6 at a concentration of 0.5 mg/ml. DAPI staining was applied to visualize the overall tissue structure (A, C, E, and G). A mouse IgA isotype standard mAb, M18-254^{FITC} (BD-PharMingen), was utilized as a background control in each staining (data not shown).

acetylglucosamine (GalNAc(4S)) joined by β 1-4 linkage to iduronic acid (IdoA)³¹, has no similarity to $\alpha(1,6)$ dextran. Considering the heterogeneity of sequences and of the terminal monosaccharides in the mammalian glycoconjugates, the cross-reactivities observed may be attributed to the binding of its nondominant structures. Alternatively, other mucosa-derived substances might exist in the CS-B preparation, either from the host cells or produced by resident microorganisms in the gut.

Because the antibody cross-reactivity to the CS-B preparation was observed by an *in vitro* carbohydrate microarray assay, we performed further experiments using *in vivo* material to critically evaluate its possible biological significance. We stained mouse intestinal tissue sections with the groove-type anti- $\alpha(1,6)$ dextran 4.3F1 (IgG3) to see whether host cells express cross-reactive molecules that interact with the antibody. To our surprise, the anti- $\alpha(1,6)$ dextran mAb 4.3F1 clearly identified a population of mononuclear cells in the lamina propria of small intestine (Fig. 4B, E). These cells are a subpopulation of monocyte/macrophages, which express CD11b/MAC1 (Fig. 4C) and are negative for CD5 (Fig. 4F), MAC3, CD19, B220, CD3, CD4, CD8, TCR- α , TCR- β , and Syndecan 1 (data not shown). This staining cannot be blocked by pretreatment of the tissue section with dextranase (Fig. 4G–I), suggesting that trapping of microbial polysaccharide dextran by these cells is most unlikely. In addition, a population of MAC1⁺ and 4.3F1⁺ cells was also detected in the small intestine of newborn mice that have not been exposed to microbial antigens (Fig. 4J–L). We conclude that the structure recognized by the groove-type anti- $\alpha(1,6)$ dextran mAb is an endogenous cellular element.

To further investigate the specificity of this antigenic cross-reactivity, we introduced an additional anti- $\alpha(1,6)$ dextran antibody, 45.21.1, in this study. 45.21.1 is a groove-type anti- $\alpha(1,6)$ dextran of IgA isotype, whose Ig-V region amino acid sequences (V_H-D-J_H and V_K-J_K) are 99% identical to those of the IgG3 anti- $\alpha(1,6)$ dextran 4.3F1 (ref. 20). The combining-site immunochemical characteristics of 45.21.1 are very similar to mAb 4.3F1, being a high-affinity anti- $\alpha(1,6)$ dextran mAb with K_a values of 2.09×10^{-5} ml/g and 1.78×10^{-4} ml/g for $\alpha(1,6)$ dextran B512 and oligosaccharide IM7, respectively^{20,32}. As we expected, this antibody also cross-reacts with CS-B on microarray (data not shown). Mouse intestinal tissue sections were then stained with either 45.21.1 (groove-type and IgA isotype) or 16.4.12E (cavity-type and IgA isotype). We reasoned that if the recognition of Dex-Ids is epitope-specific, the groove-type but not the cavity-type mAb would react with the MAC1⁺ and 4.3F1⁺ cell population

in the lamina propria of small intestine. As shown in Figure 5, these cells were indeed heavily stained by mAb 45.21.1 (Fig. 5E, F). By contrast, the cavity-type mAb 16.4.12E stained a distinct cell surface substance, which is expressed or secreted by the intestinal epithelial cells with an enriched distribution in the crypt of small intestine of adult mice (Fig. 5A, B). In addition, we showed that the immunohistological stainings of 16.4.12E and 45.21.1 were significantly inhibited by an isomaltose oligosaccharide IM6 (Fig. 5D, H).

Taken together, these investigations confirm the carbohydrate microarray finding that anti- $\alpha(1,6)$ dextran mAbs cross-react with endogenous cellular elements and demonstrate the presence of at least two types of cellular elements that mimic either the internal chain structure or the nonreducing end epitope of $\alpha(1,6)$ dextran. Expression of a $\alpha(1,6)$ dextran-like carbohydrate structure by mammalian cells is, however, highly unexpected. It is generally believed that glucose residues are present in newly synthesized but not in the mature glycoproteins in eukaryotic cells^{33,34}. The structural basis of such cross-reactivities remains to be determined. Nevertheless, recognition of the Dex-Ids at the level of immunological specificity is important because it opens the way to investigate whether and how the expression of an endogenous cellular element influences the immune response to a microbial antigen. It has been recognized for decades that murine and human immune responses to microbial polysaccharides, including $\alpha(1,6)$ dextran, are immature at the early stage of their life^{14,35}. The underlying molecular and cellular mechanisms are largely unknown. Further investigation will strive to determine whether the endogenous early expression of the Dex-Id plays a negative regulatory role in the maturation of mouse anti-dextran response and how such inhibition is released later with the presence of Dex-Id in adulthood.

In summary, we present a simple and efficient procedure for producing a carbohydrate microarray. In the current platform, about 20,000 microspots of antigens can be printed on a single microarray slide, reaching the capacity to include most known human microbial pathogens, autoantigens, and tumor-associated antigens. The detection system is highly sensitive and efficient. A broad spectrum of antibody specificities can be monitored with as little as a few microliters of serum specimen. This carbohydrate microarray platform is thus readily applicable to biomedical research on carbohydrate-based molecular recognition and to clinical diagnosis of infectious diseases and other diseases. Potential uses of this technology include the development of specialized biochips for characterizing the diversity of HIV-1 infection and host responses; probing the repertoire of opportunistic pathogens that are frequently associated with acquired immune deficiency syndrome, cancers, and other diseases with immune deficiency; and the establishment of an antigen microarray of large capacity and diversity for monitoring a wide range of microbial infections, which would enable a rapid detection of potential biological warfare.

Experimental protocol

Carbohydrate antigens and antibodies. Carbohydrate-containing macromolecules applied in Figures 2 and 3, and anti- $\alpha(1,6)$ dextran mAbs, 16.4.12E (IgA/kappa)²¹, 4.3.F1 (IgG3/kappa)²⁰, and 45.21.1 (IgA/kappa)³², were adopted from the collection of the late Professor Elvin A. Kabat of Columbia

University. (For detailed information, see Supplementary Table 1 in the Web Extras page of *Nature Biotechnology* online.). Purified proteins of 4.3F1, 45.21.1 and 16.4.12E were obtained by a procedure of affinity purification as described³⁶. The biotinylated or FITC-conjugated anti-dextran antibodies were prepared in our laboratory following standard protocols³⁷. The FITC-conjugated $\alpha(1,6)$ dextran of molecular weight 20 kDa, 70 kDa, and 2,000 kDa, FITC-inulin, a biotinylated anti-human IgG antibody, an alkaline phosphatase-conjugated anti-human IgM, and streptavidin conjugates, were purchased from Sigma (St. Louis, MO). Antibodies for cell type/lineage analysis, including antibodies specific for murine CD11b/MAC1, MAC3, TCR- α , TCR- β , CD3, CD4, CD5, CD8, CD19, B220, Syndecan-1, a mouse IgG3 isotype standard (A12-3), and a streptavidin conjugate of Texas Red, were from BD-PharMingen (San Diego, CA). A streptavidin-Cy3 conjugate was purchased from Amersham Pharmacia (Piscataway, NJ), and a red fluorescence substrate of alkaline phosphatase, Vector Red, from Molecular Probes, Inc. (Burlingame, CA).

Printing carbohydrate microarrays. A high-precision robot designed to produce cDNA microarrays (GMS 417 Arrayer; Genetic Microsystems, Inc., Woburn, MA) was utilized to spot carbohydrate antigens onto the glass slides precoated with nitrocellulose polymer (FAST Slides; Schleicher & Schuell, Keene, NH). Carbohydrate antigens were dissolved in saline (0.9% NaCl) in concentrations as specified in the figure legends. They were printed with spot sizes of $\sim 150 \mu\text{m}$ and at $375\text{-}\mu\text{m}$ intervals, center to center. The printed carbohydrate microarrays were air-dried and stored at room temperature without desiccant before application.

Staining and scanning of carbohydrate microarrays. Immediately before use, the printed carbohydrate microarrays were rinsed with PBS, pH 7.4, with 0.05% (vol/vol) Tween 20 and then blocked by incubating the slides in 1% (wt/vol) BSA in PBS containing 0.05% (wt/vol) NaN_3 at 37°C for 30 min. They were then incubated at room temperature with antibodies at an indicated titration in 1% (wt/vol) BSA in PBS containing 0.05% (wt/vol) NaN_3 and 0.05% (vol/vol) Tween 20. Application of secondary antibodies or streptavidin conjugates is specified in figure legends. The stained slides were rinsed five times with PBS with 0.05% (vol/vol) Tween 20, air-dried at room temperature, and then scanned for fluorescent signals. The stained microarrays were scanned with a ScanArray 5000 Standard Biochip Scanning System (Packard BioChip Technologies, Inc., Billerica, MA) and data analyzed using QuantArray version 2.1 software associated with the system.

ELISA and in situ immunofluorescence. ELISA and immunofluorescence staining were carried out as described^{21,38}. The dextranase treatments were performed by a preincubation of tissue sections with dextranase (Sigma) at 0.5 unit/ml in 100 mM potassium PBS, pH 6.0, 37°C for 60 min. This condition allows a complete removal of molecules of FITC- $\alpha(1,6)$ dextran that were specifically trapped by immune cells in the spleen sections of a $\alpha(1,6)$ dextran-immunized mice³⁸.

Note: Supplementary information can be found on the Nature Biotechnology website in Web Extras (http://biotech.nature.com/web_extras).

Acknowledgments

We acknowledge the late Professor Elvin A. Kabat and his previous students, postdoctoral fellows, and collaborators for their contributions to the collection of carbohydrate antigens and antibodies that were applied in this study. This work is supported by research grants of NIH (AI45326) and Compass Pacific to D.W.

Received 17 July 2001; accepted 28 December 2001

1. Feizi, T. The antigens Ii, SSEA-1 and ABH are in interrelated system of carbohydrate differentiation antigens expressed on glycosphingolipids and glycoproteins. *Adv. Exp. Med. Biol.* **152**, 167–177 (1982).
2. Crocker, P.R. & Feizi, T. Carbohydrate recognition systems: functional triads in cell–cell interactions. *Curr. Opin. Struct. Biol.* **6**, 679–691 (1996).
3. Focarelli, R., La Sala, G.B., Balasini, M. & Rosati, F. Carbohydrate-mediated sperm–egg interaction and species specificity: a clue from the *Unio elongatulus* model. *Cells Tiss. Org.* **168**, 76–81 (2001).
4. Rosati, F., Capone, A., Giovampaola, C.D., Brettoni, C. & Focarelli, R. Sperm–egg interaction at fertilization: glycans as recognition signals. *Int. J. Dev. Biol.* **44**, 609–618 (2000).
5. Feizi, T. Progress in deciphering the information content of the 'glycome'—a crescendo in the closing years of the millennium. *Glycoconj. J.* **17**, 553–565 (2000).
6. Feizi, T. Carbohydrate-mediated recognition systems in innate immunity. *Immunol. Rev.* **173**, 79–88 (2000).
7. Hakomori, S. Aberrant glycosylation in cancer cell membranes as focused on glycolipids: overview and perspectives. *Cancer Res.* **45**, 2405–2414 (1985).
8. Sell, S. Cancer-associated carbohydrates identified by monoclonal antibodies. *Hum. Pathol.* **21**, 1003–1019 (1990).
9. Adachi, M. *et al.* Expression of Le^x antigen in human immunodeficiency virus-infected human T cell lines and in peripheral lymphocytes of patients with acquired immune deficiency syndrome (AIDS) and AIDS-related complex (ARC). *J. Exp. Med.* **167**, 323–331 (1988).
10. Nakaiishi, H., Sanai, Y., Shibuya, M., Iwamori, M. & Nagai, Y. Neosynthesis of neo-lacto- and novel ganglio-series gangliosides in a rat fibroblastic cell line brought about by transfection with the v-fes oncogene-containing Gardner–Arnstien strain feline sarcoma virus-DNA. *Cancer Res.* **48**, 1753–1758 (1988).
11. Schachter, H. & Jaeken, J. Carbohydrate-deficient glycoprotein syndrome type II. *Biochim. Biophys. Acta* **1455**, 179–192 (1999).
12. Karlsson, K.A., Angstrom, J., Bergstrom, J. & Lanne, B. Microbial interaction with animal cell surface carbohydrates. *APMIS Suppl.* **27**, 71–83 (1992).
13. Feizi, T. & Loveless, R.W. Carbohydrate recognition by *Mycoplasma pneumoniae* and pathologic consequences. *Am. J. Respir. Crit. Care Med.* **154**, S133–S136 (1996).
14. Wang, D. & Kabat, E.A. Carbohydrate antigens (polysaccharides) In *Structure of antigens*, Vol. 3. (ed. M.H.V.V. Regenmortel) 247–276 (CRC Press, Boca Raton FL; 1996).
15. Finne, J., Leinonen, M. & Makela, P.H. Antigenic similarities between brain components and bacteria causing meningitis. Implications for vaccine development and pathogenesis. *Lancet* **2**, 355–357 (1983).
16. Mandrell, R.E. *et al.* Lipooligosaccharides (LOS) of some *Haemophilus* species mimic human glycosphingolipids, and some LOS are sialylated. *Infect. Immun.* **60**, 1322–1328 (1992).
17. Wang, D. *et al.* The repertoire of antibodies to a single antigenic determinant. *Mol. Immunol.* **28**, 1387–1397 (1991).
18. Jeanes, A. Immunochemical and related interactions with dextrans reviewed in terms of improved structural information. *Mol. Immunol.* **23**, 999–1028 (1986).
19. Cisar, J., Kabat, E.A., Dörner, M.M. & Liao, J. Binding properties of immunoglobulin combining sites specific for terminal or nonterminal antigenic determinants in dextran. *J. Exp. Med.* **142**, 435–459 (1975).
20. Wang, D. *et al.* Two families of monoclonal antibodies to $\alpha(1,6)$ dextran, V_H19.1.2 and V_H9.14.7, show distinct patterns of J_H and J_H minigene usage and amino acid substitutions in CDR3. *J. Immunol.* **145**, 3002–3010 (1990).
21. Matsuda, T. & Kabat, E.A. Variable region cDNA sequences and antigen binding specificity of mouse monoclonal antibodies to isomaltosyl oligosaccharides coupled to proteins. T-dependent analogues of $\alpha(1,6)$ dextran. *J. Immunol.* **142**, 863–870 (1989).
22. Chen, H.T., Makover, S.D. & Kabat, E.A. Immunochemical studies on monoclonal antibodies to stearyl-isomaltotetraose from C58/J and a C57BL/10 nude mouse. *Mol. Immunol.* **24**, 333–338 (1987).
23. Kabat, E.A. *et al.* Human monoclonal macroglobulins with specificity for *Klebsiella* K polysaccharides that contain 3,4-pyruvylated-D-galactose and 4,6-pyruvylated-D-galactose. *J. Exp. Med.* **152**, 979–995 (1980).
24. Kabat, E.A., Liao, J., Sherman, W.H. & Osserman, E.F. Immunochemical characterization of the specificities of two human monoclonal IgMs reacting with chondroitin sulfates. *Carbohydr. Res.* **130**, 289–297 (1984).
25. Kabat, E.A. *et al.* The epitope associated with the binding of the capsular polysaccharide of the group B meningococcus and of *Escherichia coli* K1 to a human monoclonal macroglobulin, IgM^{NOV}. *J. Exp. Med.* **168**, 699–711 (1988).
26. Liao, J. *et al.* Characterization of a human monoclonal immunoglobulin M (IgM) antibody (IgM^{BE_N}) specific for Vi capsular polysaccharide of *Salmonella typhi*. *Infect. Immun.* **63**, 4429–4432 (1995).
27. Avrameas, S. Multispecific antibodies. *Int. Rev. Immunol.* **3**, 1–146 (1988).
28. Herzenberg, L.A. & Herzenberg, L.A. Toward a layered immune system. *Cell* **59**, 953–954 (1989).
29. Thompson, K.M. *et al.* Human monoclonal antibodies specific for blood group antigens demonstrate multispecific properties characteristic of natural autoantibodies. *Immunology* **76**, 146–157 (1992).
30. Thorpe, S.J. *et al.* Human monoclonal antibodies encoded by the V4-34 gene segment show cold agglutinin activity and variable multireactivity which correlates with the predicted charge of the heavy-chain variable region. *Immunology* **93**, 129–136 (1998).
31. Leteux, C. *et al.* The cysteine-rich domain of macrophage mannose receptor is a multispecific lectin that recognizes chondroitin sulfates A and B and sulfated oligosaccharides of blood group Lewis^a and Lewis^x types in addition to the sulfated N-glycans of lutropin. *J. Exp. Med.* **191**, 1117–1126 (2000).
32. Sharon, J., Kabat, E.A. & Morrison, S.L. Association constants of hybridoma antibodies specific for $\alpha(1\rightarrow6)$ linked dextran determined by affinity electrophoresis. *Mol. Immunol.* **19**, 389–397 (1982).
33. Spiro, R.G. Glucose residues as key determinants in the biosynthesis and quality control of glycoproteins with N-linked oligosaccharides. *J. Biol. Chem.* **275**, 35657–35660 (2000).
34. Zuber, C., Spiro, M.J., Guhl, B., Spiro, R.G. & Roth, J. Golgi apparatus immunolocalization of endomannosidase suggests post-endoplasmic reticulum glucose trimming: implications for quality control. *Mol. Biol. Cell* **11**, 4227–4240 (2000).
35. Howard, J. T cell-independent responses to polysaccharides: their nature and delayed ontogeny In *Towards better carbohydrate vaccines*. Proceedings of a meeting organized by the World Health Organization, 9–11 October 1986, Geneva. (eds Bell, R. & Torrigiani, G.) 221–229 (John Wiley & Sons, New York, NY; 1987).
36. Lai, E. & Kabat, E.A. Immunochemical studies of conjugates of isomaltosyl oligosaccharides to lipid: production and characterization of mouse hybridoma antibodies specific for stearyl-isomaltosyl oligosaccharides. *Mol. Immunol.* **22**, 1021–1037 (1985).
37. O'Shannessy, D.J., Dobersen, M.J. & Quarles, R.H. A novel procedure for labeling immunoglobulins by conjugation to oligosaccharide moieties. *Immunol. Lett.* **8**, 273–277 (1984).
38. Wang, D., Wells, S.M., Stall, A.M. & Kabat, E.A. Reaction of germinal centers in the T-cell-independent response to the bacterial polysaccharide $\alpha(1\rightarrow6)$ dextran. *Proc. Natl. Acad. Sci. USA* **91**, 2502–2506 (1994).